Review of transmission scanning configurations in cardiac SPECT

Mahsa Noori Asl and Alireza Sadremomtaz

Department of Physics, Faculty of Sciences, University of Guilan, Rasht, Iran

ABSTRACT

The diagnostic accuracy of single photon emission computed tomography (SPECT) is profoundly influenced by attenuation phenomenon. Soft tissue attenuation degrades cardiac SPECT image quality, thereby decreasing the possibility of the detection of the lesions. A variety of correction techniques based on different assumptions have been used to reduce the impact of attenuation. Several types of systems with different transmission hardware modifications and external sources have been developed for clinical implementation. Each system has unique advantages and limitations. In this study, firstly, we introduce the attenuation phenomenon, the problems arising from it and the attenuation correction methods with description of the assumptions related to each of them. The main purpose of this study is to review the developments in the field involving various configurations used for attenuation correction of SPECT images, as tested using either phantom or clinical data, and to delineate an optimal attenuation correction technique by considering the advantages and limitations with each of the configurations.

Key words: SPECT; Attenuation; Emission data; Transmission data; Correction factor

Corresponding author: Mahsa Noori Asl, PhD Student, Department of Physics, Faculty of Sciences, University of Guilan, Rasht, Iran. E-mail: nooriasl.mahsa@gmail.com

1. Introduction

The physical basis of attenuation lies in this fact that photons emitted from injected radiopharmaceutical, as passing through the body, interact with the different tissues. As a result of these interactions, a number of photons may be absorbed or scattered away from the detectors, thus not detected, or may be scattered and detected in different detectors, complicating the reconstruction task [1]. Therefore, attenuation may result in artifacts, inaccuracies and also reduction of contrast in reconstructed images. These are particularly of important in myocardial perfusion imaging (MPI) because the thorax region contains highly nonuniform distribution of the tissues (e.g., bone tissues, soft tissues and lungs). Thereby, the use of accurate attenuation correction, especially for imaging of the thorax region, is of utmost importance [2].

Two classes of methods have been developed to calculate the attenuation map in clinical practice: calculated and measured attenuation correction methods. The first class of methods, assuming a uniform attenuation throughout the patient, is appropriate for brain studies. But for areas of inhomogeneous attenuation such as the chest, these approximate methods cannot compensate for nonuniform attenuation [3]. Measured attenuation correction methods overcome this problem and use attenuation maps obtained by using of various transmission scanning systems and external sources. This paper describes the physical basis of attenuation correction methods and summarizes recent protocols developed to compute the attenuation correction map using the transmission data in cardiac SPECT imaging.

2. Attenuation phenomenon and the problems arising from it

Attenuation results from different interactions that a photon may undergo when it passes through an absorber media. Among these interactions, two interactions are of most importance in the photon energy range of interest in nuclear medicine (i.e., 68-80 keV for ^{201}Tl to 511 keV for positron emitters): the photoelectric effect in which the primary photon is completely absorbed, and the Compton scattering in which direction of the photon motion and its energy change. The total probability for interaction μ, called the total linear attenuation coefficient that is equal to the sum of the probabilities of these two interactions [4].

If a narrow-beam of monoenergetic photons passes through an absorber of thickness t, then the transmitted beam intensity, I(t), is given by the following exponential relationship:

$$I(t) = I_0 \exp\left(-\int_0^t \mu_t(x,y)dl\right)$$
(1)

where I_0 is the beam intensity without absorber, and $\mu_t(x,y)$ is the total linear attenuation coefficient in the differential distance dl [1, 5].

One of the major problems arising from attenuation in SPECT imaging is that the photons emitted from radiopharmaceutical in deeper structures of the organ being imaged have to pass through more tissue to reach the detector. Thereby, these photons undergo more attenuation than those emitted near the edges. For this reason, in the reconstructed image of the organ, the central structures show artificially decreased radioactivity than the outer contour and therefore they seem dark (see Figure 2-A) [6].

In medical imaging, the artifacts created by attenuation may be confused with true lesions. Therefore, the use of the attenuation correction methods is necessary to increase image quality and improve diagnostic accuracy.

3. Attenuation correction

The two general methods [7-9] commonly used for attenuation correction are based on two opposing assumptions:

1. The attenuating media can essentially be considered uniform. Therefore, a constant and spatially independent μ_t can be used throughout the organ being imaged.

2. The attenuating media has been made of the different tissues. Therefore, each part of the organ has an individual linear attenuation coefficient and tissue attenuation is highly spatially dependent. Thereby, $\mu_t(l)$ cannot be considered a constant value.

In the first situation, the method used for attenuation correction is known as the Chang method, and in latter, as the transmission scanning or transmission source method.

3.1. The Chang method (calculated attenuation correction)

The Chang algorithm [10], as shown in Figure 1, is based on FBP reconstruction of a point source located inside an attenuating media of a constant attenuation coefficient and a known shape. In this method, attenuation correction factor is calculated from the average attenuation of photons traveling from each point in the organ of interest at different projection angles [7].

This correction factor takes into account source depth and the tissue attenuation coefficient [11].
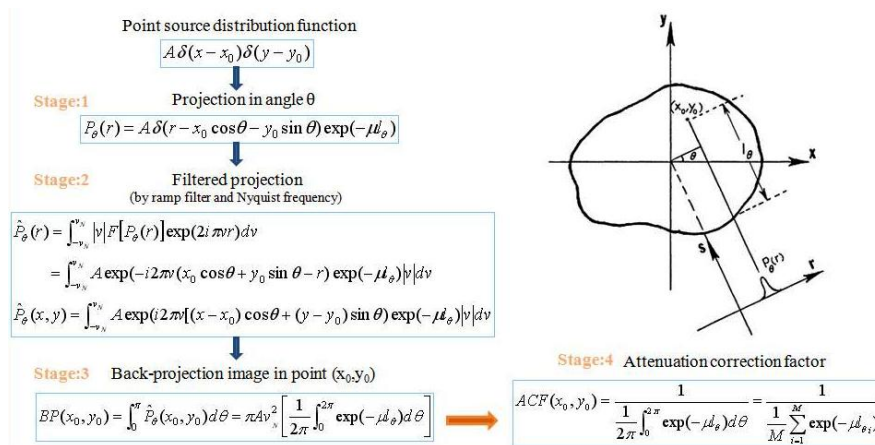
Fig 1. Illustration of the derivation of the Chang correction factor based on FBP reconstruction of a point source (the Chang algorithm). Firstly, a projection of the point source in angle θ is calculated. Then, the filtered projection at this angle is given by ramp filter, $|v|$, and Nyquist frequency, v_N. In the next stage, the FBP reconstruction of the point source in point (x_0,y_0) is performed. Finally, from the reconstructed image by FBP method, it can be resulted easily that the effect of attenuation can be eliminated by using of a correction factor $ACF(x_0,y_0)$ that has been given in stage4 [10].

In the Chang method, determination of correct organ boundary is of most important. For this purpose, a reconstructed image without correction from the organ being imaged is used to estimate the outline and thereby the distance that the photons have to travel within the organ [6]. Then a correction factor map, based on estimated organ boundary and a constant μ_t, is generated and applied to the reconstructed transverse slices [8, 9]. Using this map, a high scaling factor at the middle and lower scaling factor to the edges is applied to the emission image and thus, darkness arising from attenuation in the middle of the image is eliminated. However, this correction method will only work reasonably well for the organs such as brain or abdomen, where μ_t is approximately constant [6, 7].

3.2. The transmission source method (measured attenuation correction)

When the attenuating media is nonuniform (e.g. cardiac studies), another attenuation correction method, that uses a variable attenuation coefficient dependent on the spatial location of the pixel in the patient, is required [8]. In this situation, the attenuation correction is performed using the images obtained from two scans [12]:

1. *The blank scan*:

The data of this scan contain the photons acquired from the used external source without the patient in the scanner.

2. *The transmission scan*:

The data of this scan contain the photons acquired from the used external source as passing through the body of patient.

The ratio of counts of each pixel (i, j) between the blank scan image (I_{Blank}) and the transmission scan image (I_{Trans}) gives the attenuation correction factor (ACF) for the pixel:

$$ACF(i,j) = \frac{I_{Blank}(i,j)}{I_{Trans}(i,j)} \qquad (2)$$

This equation results in an attenuation correction map that is applied on the pixel data of the emission scan for obtaining the corrected image [9].

In this correction method, the data acquired from a blank scan can be used for all subsequent patients during the day. But the data of the transmission and emission scan, that should be performed individually for any patient, can be acquired in three ways [12, 13]:

1. *Sequential Acquisitions*, where a separate tomographic scan is performed for each emission and transmission scan.

2. *Simultaneous Acquisitions*, where both the emission and transmission images are acquired simultaneously per projection angle and in one tomographic rotation.

3. *Simultaneous Interleaved Acquisitions*, where both the emission, and transmission images are acquired sequentially per each projection angle and in one tomographic rotation.

Advantages and disadvantages of each method are listed in Table 1.

Table 1: Comparison of the acquisition methods [12].

Method	Advantages	Disadvantages
Sequential	-Uncontaminated data	-Timing: two separate scan -Possibility of patient motion between two scan
Simultaneous	-Timing: as much as only one emission scan Reduction of patient motion error (data registration in the same time)	-Contamination of emission data with transmission data
Simultaneous interleaved	-Data acquisition during one scan -Reduction of patient motion error (data registration in very closely spaced in time) -Reduction of contaminated data	-Timing: more than only one emission scan

Table 2: Isotopes used commonly for performing low-energy transmission tomography [5].

Isotope	Decay mode	Photon emissions energy (keV) and (yield)	K shell x-ray emissions energy(key) and (yield)	Half-life
^{241}Am	α	59.4 (35.9%)	-	432.2 yr
^{153}Gd	EC	97.4 (27.6%), 103.2(19.6%)	40.9-48.3 (118.6%)	241.6 days
^{133}Ba	EC	356.01(62.05%), 302.85 (18.33%)	-	10.54 yr
^{201}Tl	EC	135.3 (2.65%), 167.4 (10.0%)	68.9-82.6 (93.8%)	73.1 hr
^{99m}Tc	IT	140.5 (89.1%)	18.2-20.6 (5.77%)	6.01 hr

EC= electron capture and IT = isomeric transition.

One of the important points in the use of the simultaneous transmission-emission scan for attenuation correction is the choice of an appropriate isotope as the transmission source. This isotope should be chosen to minimize crosstalk between the transmission and emission energy windows. Crosstalk occurs when the scattered photons from the higher energy isotope fall into the energy window of the lower energy isotope. Since the common radiopharmaceuticals used for cardiac SPECT imaging contain ^{201}Tl or ^{99m}Tc isotope, in order to minimize crosstalk in emission data, the photon energy of the transmission isotope usually are chosen to be less than the photon energy of these two emission isotopes. Also, to eliminate periodic refilling or replacement of the transmission sources, these isotopes usually are of a long half-life. A number of common isotopes used for emission and transmission tomography are given in Table 2. It may seem that the use of the sequential acquisition mode is more appropriate than simultaneous mode, because in this acquisition method, the transmission scan is performed before the emission scan and therefore, the problem of the contamination of the transmission and emission data is eliminated. But, it should be noted that the sequential mode increases imaging time,

thereby increasing the probability of patient motion between the two scan. The patient motion will result in problems in the spatial alignment of the two data sets, thereby introducing errors into the attenuation corrected images [3, 14].

Since transmission photon energy is different from the energy of photons emitted from injected radiopharmaceutical, therefore, a scaling factor must be applied to convert the attenuation coefficient of the transmission source energy to that of injected radiopharmaceutical. Based on a method that is commonly used, μ_t varies linearly between the emission (E_e) and transmission (E_t) energies, and thus, the measured transmission attenuation coefficients $\mu_t(E_t)$ can be related to the emission attenuation coefficients $\mu_t(E_e)$ using the following equation:

$$\mu_t(E_e) = \frac{\mu_t^{tis}(E_e)}{\mu_t^{tis}(E_t)} \mu_t(E_t)$$

(3)

where $\mu_t^{tis}(E_e)$ and $\mu_t^{tis}(E_t)$ are the linear attenuation coefficients of tissue for the emission and transmission isotopes, respectively [5].

The accuracy of attenuation correction by using of the transmission source method depends on the type

of the used transmission source, lack of patient motion, and also the geometry used for the attenuation correction. Several groups of the investigators has studied the effect of attenuation correction for cardiac SPECT using single-, dual- and triple-head SPECT cameras and different configurations of the transmission sources. Here, we review a number of these studies with the results.

4. Different geometries used for transmission scan

4.1. A triple-detector SPECT system with a fixed line source

In this protocol, a line source as the transmission source is placed at the focal line of one of the three detectors (see Figure 2).
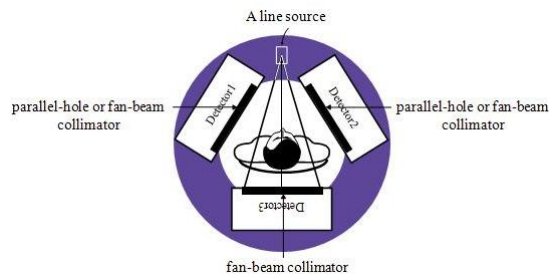

Fig 2. Geometry used for a simultaneous transmission-emission scan using a triple-head camera and a fixed line source that was placed along the focal line of the opposite detector. This detector always is equipped with a fan-beam collimator, for elimination of the scattered photons from external source, but the other two detectors may be equipped with parallel-hole or fanbeam collimators [12].

By using of a simultaneous transmission-emission scan, the detector opposite to the line source collects combined transmission-emission data, and the remaining two detectors collect only emission data. For rejection of the transmission photons that are scattered in the body of the patient, this detector usually is equipped with a fan-beam collimator. But, based on the studies performed for attenuation correction, two "emission only" detectors may be equipped with parallel-hole or fan-beam collimators. Also, each detector acquire two data sets in two different energy windows: one centered on the emission photopeak and other centered on the transmission photopeak.

This protocol was used by *Ficaro et al*. for the first time [5]. In this study, the ability of ^{241}Am and ^{99m}Tc was compared for using as transmission sources for attenuation correction of ^{201}Tl cardiac SPECT imaging. In two separate tests, these collimated line sources have been placed opposite and parallel to detector 3 of a PRISM 3000 SPECT system (Picker-Ohio Imaging, Nuclear Medicine Division of Picker

International) equipped with a LEGP fan-beam collimator with a focal length of 65 cm. Instead of fan-beam collimators, detector 1 and 2 were equipped with LEHR parallel-hole collimators to minimize contamination of the emission and transmission data and also truncated collection of the emission data.

The results obtained from this investigation showed that for detector 1, contamination from ^{201}Tl in the ^{241}Am energy window was approximately five times greater than the ^{99m}Tc energy window, while the contamination from ^{99m}Tc in the ^{201}Tl data was approximately five times greater than ^{241}Am. Instead, for detector 1 and 2, no contamination was detected in the ^{201}Tl data from ^{241}Am, whereas the ^{99m}Tc resulted in a small crosstalk component. Also, the low energy of photons emitted from ^{241}Am results in more bone-tissue contrast than ^{99m}Tc and despite the higher activities needed to achieve transmission rates comparable to ^{99m}Tc, the whole-body, absorbed dose is lower. From these results, they concluded that ^{241}Am is a more convenient transmission source than ^{99m}Tc for simultaneous acquisition mode and result in higher signal-to-crosstalk ratios for ^{201}Tl studies.

Based on the findings of this study, ^{241}Am was used as transmission source for other 2 studies with the same configurations of above trial for evaluation of the effect of attenuation correction on: 1) ^{201}Tl cardiac perfusion SPECT images (on 40 patients and 10 normal volunteers) [14], and 2) stress ^{99m}Tc-sestamibi cardiac SPECT images (on 60 patients and 59 normal volunteers) [15]. The results of these studies showed that attenuation correction results in effective elimination of attenuation artifacts from reconstructed images and thereby improving significantly specificity without a loss in sensitivity. Therefore, these investigators concluded that the use of attenuation correction for MPI is necessary to improve image information for diagnosing coronary heart disease (CHD).

Matsunari et al. [16, 17] used a triple-head SPECT system (MULTISPECT 3, Siemens AG, Erlangen, Germany) fitted with a low-energy, fan-beam collimator with a focal length of 53 cm for detector 1 and with LEHR parallel-hole collimators for detector 2 and 3. The transmission source consisted of a ^{241}Am line source sealed in a stainless-steel tube.

The aims of these studies were to 1) compare the distribution of the normals between attenuation-corrected rest ^{201}Tl and stress ^{99m}Tc-sestamibi SPECT images (on 21 patients with low likelihood of CAD), 2) evaluate the effect of attenuation correction on ^{99m}Tc-tetrofosmin SPECT images for detecting viable myocardium in compared with FDG PET (on 24 patients (21 males and 3 females) with CAD). The first study showed that, a significant difference exists in normal count density distribution between attenuation-corrected ^{99m}Tc-sestamibi and ^{201}Tl

SPECT images. The results of the second study indicated that attenuation correction improves the detection of viable myocardium mainly by decreasing the underestimation of viability in the inferior-septal region. However, the AC ^{99m}Tc-tetrofosmin SPECT may, still underestimate and/or overestimate myocardial viability in compared with FDG PET.

In the other experiment that has been performed by *Vidal et al*. [18], the impact of attenuation correction was investigated on the visual interpretation of [201]T1 stress/4 h-delayed cardiac images for patients with various degrees of CAD. In this study, a Picker Prism 3000 XP triple-head camera (Picker International, Cleveland, OH) equipped with a LEHR fanbeam collimator for each detector was used. The transmission source was a shielded, shuttered and collimated ^{99m}Tc line source.

In this investigation, 56 patients (22 normal patients and 19, 13 and 2 patients with one-, two- and three-vessel disease, respectively) were studied. The results obtained from this study indicated that attenuation correction affects significantly on the visual interpretation of stress/4 h delayed cardiac SPECT and the specificity of defect detection is increased significantly in the inferior wall (right coronary artery (RCA) region), whereas the sensitivity of defect detection is significantly reduced in the anteroseptal (the left anterior descending artery (LAD)) regions.

4.2. A 90° dual-head SPECT system with two scanning line sources

In this protocol, a dual-head camera, in which two heads were separated by 90 degrees, was used. Two identical line sources are mounted on the gantry opposite to each detector and were moved mechanically at constant speed along the planes parallel to each detector surface (see Figure 3).
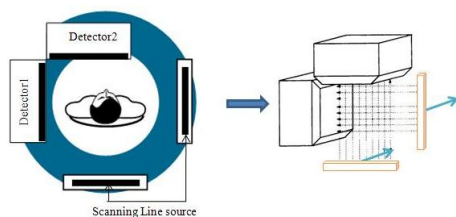

Fig 3. Geometry used for a dual-head camera with two scanning line sources. Each line source moves away from the gantry during one transmission acquisition and then towards the gantry on the next acquisition and thereby providing the transmission data required to produce attenuation map [12, 37].

In this protocol, the transmission and emission data were commonly acquired by simultaneous or simultaneous interleaved mode and with the same parallel-hole collimators. The transmission data

usually were acquired in an electronically controlled window moving synchronously with the line source over the detector. This provides the possibility of the simultaneous acquisition of emission data outside the window 5using different energy channels.

This protocol was used by *Kluge et al*. [19], for determination of the clinical advantages of attenuation correction in improvement of diagnostic accuracy of CAD using ^{99m}Tc-tetrofosmin in 50 males (25 normals and 25 patients). In this study, a dual-head camera (ADAC Laboratories, Vertex) equipped with ultra-high-resolution collimators and two [153]Gd line sources were used. The line source was physically collimated and opened only during acquisition so that there was only minimal radiation exposure to the patient. In each projection angle, emission and transmission data were acquired simultaneously. The limitations of this investigation were the use of different reconstruction algorithms for NC and AC studies, the absence of a scatter correction method, and study only on male patients. The results indicated that attenuation correction increases diagnostic accuracy (specificity and sensitivity) as evaluating infero-posterior wall segments.

In the study performed by *Gallowitsch et al*. [20, 21] the effect of attenuation correction on the ^{201}Tl SPECT images using two moving collimated [153]Gd line source was investigated in a group of patient with different degrees of CAD. In these studies, a dual-detector system (Apex SP-X Cardia-L, Elscint) fitted with a low-energy all-purpose (LEAP) parallel-hole collimator was used and the emission and transmission data were acquired simultaneously. The results showed that attenuation correction performed by this protocol is feasible in patients with different degrees of CAD and significantly affects on the diagnostic accuracy of the severity and extent of CAD.

In the study by *Almquist et al*. [22], attenuation correction was performed by a dual-head gamma camera (Genesys Vertex, ADAC Laboratories, Milpitas, Calif) equipped with a LEHR collimator and two scanning [153]Gd line source. The purpose of this study was to investigate quantify effects of down-scatter in attenuation-corrected images under realistic conditions. In this study, 43 patients (23 males and 23 females) were tested in a 1-day ^{99m}Tc-tetrofosmin rest-stress SPECT protocol. The results of this study demonstrated that attenuation correction of the images results in differences between the results of the rest and stress tests that weren't seen in non-corrected images. A phantom study indicated that these differences are due to different degrees of down-scatter, because of different patient doses at rest and exercise tests.

In the other study performed by *Hendel et al.* [23, 24], ^{99m}Tc-sestamibi MPI was performed with a noncircular clockwise orbit using a dual-head camera (Vertex, ADAC Laboratories). The transmission data was acquired by a shuttered moving ^{153}Gd line source and simultaneously with the emission data. A unique aspect of this study was the use of scatter correction and depth-dependent resolution compensation with the attenuation correction. The results of this investigation demonstrated that the normalcy rate of SPECT MPI is significantly improved using these combined corrections without a decline in overall sensitivity. However, there is a reduction in detection probability of extensive coronary disease.

Links et al. [25] performed attenuation, depth-dependent blur, and motion combined corrections by using of a dual-detector system (SMV DST or DST-XL) equipped with LEHR collimator. In this study, emission radionuclide used was either ^{99m}Tc or ^{201}Tl, and also transmission source was either ^{153}Gd or ^{99m}Tc. At each projection angle, acquisition of the emission and transmission data was performed by using of either simultaneous or simultaneous interleaved mode. The results of this investigation, that was performed on 112 patients (36 females and 76 males), demonstrated that use of combined corrections resulted in significant improvement of specificity and therefore, significantly improved diagnostic accuracy in MPI.

In *Harel et al.*'s study [26], imaging was performed using a double-head camera (DST; SMV International, Buc, France) equipped with LEHR parallel-hole collimators and two external shuttered moving ^{153}Gd line sources. These sources were collimated with lead shielding to produce a planar beam that yields transmission CT images. The shield door was closed during the emission acquisition to avoid downscatter of transmission source photons into the emission data. The aim of this study was to investigate clinical impact of the combined corrections (scatter, attenuation Correction and depth-dependent resolution recovery) in ^{201}Tl SPECT MPI. From the results of this study, was concluded that the use of attenuation correction combined with depth-dependent resolution recovery improves the specificity of the diagnosis of CAD whereas significantly decreases the sensitivity so that this drawback is not restored by scatter correction.

In study performed by *Gibson et al.* [27], imaging was performed by a dual head variable angle camera and using a scanning ^{153}Gd line sources that were mounted opposite to each detector (Vertex camera, Vantage ADAC, Milpitas, California). The aim of this investigation was to validate the safety of stress-only ^{99m}Tc- sestamibi SPECT imaging, employing attenuation correction in patients with low to medium probability for CAD. If the stress images, before or after attenuation correction, were interpreted as normal, the patients weren't refered to the rest imaging. The results obtained from this study showed that stress-only imaging in the patient population studied (729 patient) is a safe and valid imaging modality that results in time- and cost- saving.

In the other study, *Velidaki et al.* [28] used an L-shaped dual-head system (Optima NX, General Electric Milwaukee, USA) and two collimated ^{153}Gd line sources. In this study, emission and transmission data was acquired using simultaneous interleaved mode, and the transmission line sources were stored in a shielded parking position when they weren't used. Use of this acquisition mode resulted in reduction of crosstalk from the emission scan into the transmission image. The purpose of this investigation was to evaluate the clinical effects of attenuation and scatter correction in ^{201}Tl SPECT MPI. This study that performed on 102 patients (76 males, 26 females) demonstrated that for scatter and attenuation corrected images, the specificity for the right coronary artery territory increased significantly but a partial loss occurs in sensitivity.

4.3. A 90° dual-head spect system with multiple line sources

In *Slart et al.*'s study [29], SPECT images were acquired by using a dual-head gamma camera (Siemens E.Cam) equipped with LEHR collimators. The attenuation correction system consisted of an array of ^{153}Gd line sources incorporated in retractable 'wings' on the camera. These wings created a 180° degree arc opposite to the 90° heads (see Figure 4).
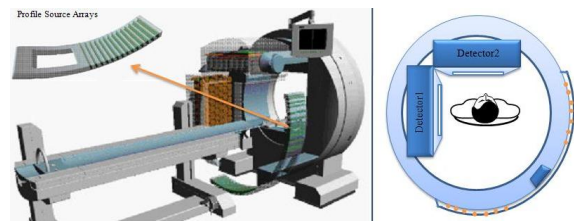

Fig 4. Geometry used for the attenuation correction by using an array of the line sources incorporated in retractable 'wings' on the system that is called 'profile attenuation correction'. These wings form a 180° degree arc opposite to the perpendicular camera heads [30].

In this study, the external sources were opened and closed by a shutter, thereby emission and transmission data could be acquired by the simultaneous interleaved mode using the two energy windows: a 20% window over the ^{99m}Tc-photopeak and a 20% window over the ^{153}Gd-photopeak. In this study, the use of an array of ^{153}Gd rods results in the production of a higher photon flux, thereby an

attenuation map with higher resolution than pervious source configurations.

The purpose of this study was to evaluate the effects of attenuation correction on MPI for a 1-year study period. The results obtained from this investigation demonstrated that, the specificity of the attenuation-corrected images, at the start of 1-year period, shows an increase in compared to the non-corrected images but the sensitivity decreases. After 1-year study, the sensitivity of corrected-images approaches to that of non-corrected images. Also, after 1-year, the sensitivity and the specificity of non-corrected images had increased as compared with those at the start of period.

4.4. A single-head SPECT system with a collimated sheet source

In the study by *Tsui et al.* [31], a ^{99m}Tc sheet source was used as the transmission source for attenuation correction of ^{201}Tl SPECT images. This study was performed on a heart-lung phantom and a patient. In order to reduce patient exposure and image degrading effects from scattered transmission photons, a special parallel-hole collimator was used to restrict these photons (see Figure 5).
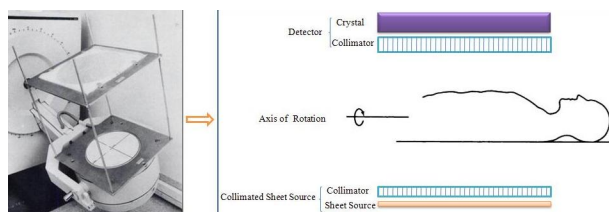

Fig 5. Schematic diagram of the transmission study setup using a ^{99m}Tc sheet source collimated by a special parallel-hole collimator to restrict the scattered emissions from the transmission sheet source and reduction of the patient exposure [31, 32].

In this study, transmission and emission scan were performed sequentially and after the transmission scan, the collimated sheet source is removed from its holder and then radiopharmaceutical is injected.

The results of the study demonstrated that attenuation correction improves image quality by reduction of statistical noise and also radioactivity distribution uniformity by more accurate quantitative information. One of the disadvantages of the protocol used in this study is that it requires a separately emission and transmission study and therefore, can require imaging times of more than an hour which is very uncomfortable for the patient. However, this avoids the contamination of the emission data by scattered data from the higher energy transmission source.

4.5. A 180° dual-head spect system with a small uncollimated sheet source

To achieve sufficiently large imaging FOV, *Kojima et al*. [33], used a 180° dual-head SPECT system (GCA 7200A, Toshiba, Japan) equipped with asymmetric fan-beam (AsF) collimator and a small uncollimated ^{99m}Tc sheet-source as transmission source for attenuation correction of ^{201}Tl images (see Figure 6-A). In this study, transmission and emission data were acquired sequentially in a cardiac phantom with a myocardial chamber and a patient study. In the patient study, after collection of the emission data, the LEGP parallel-hole collimator was removed and the AsF collimator was mounted on the detector 1. The transmission source holder including a small uncollimated ^{99m}Tc sheet source was mounted at the edge of the opposite detector. This scheme focuses on only half of the intended FOV in each projection. The right half of FOV can be sampled from this projection. The remaining half of the FOV will be sampled from an opposing projection after 180° detector rotation (see Figure 6-B).
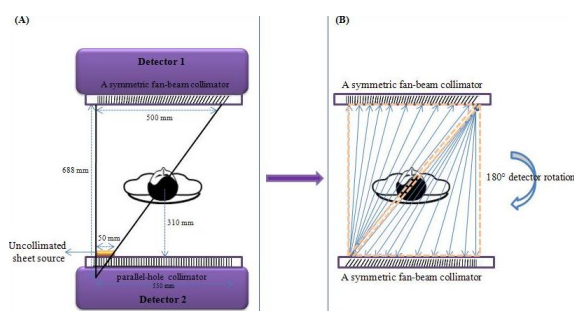

Fig 6. (A) A schematic display of the two-head SPECT system. A small uncollimated sheet source and a source holder are mounted on the edge of the Detector 2. (B) The AsF geometry and the half FOV of the SF geometry [33].

In this study, for obtaining the accurate attenuation-corrected images, three-energy windows method was used for scatter correction both ^{201}Tl and ^{99m}Tc images. Also, the use of the AsF collimator on the detector results in substantial scatter reduction in transmission data acquisition. One problem with this geometry is lower sensitivity of the AsF collimator because of the limited FOV in compared with the parallel-hole collimator. The other problem is due to non-uniformity of the periphery of the useful FOV of the detector in compared with the center of the FOV that may result in the degradation of the emission reconstructed images. Although in this protocol, the acquisition of the transmission and emission data was performed sequentially but because the transmission data was acquired in a short time, therefore, the level of patient exposure and the possibility of the patient motion between two scans are comparable with the

simultaneous mode. In addition, the results of this investigation showed that the protocol used provides accurate quantification of the ^{201}Tl radioactivity distribution in the thorax and is feasible for clinical use.

4.6. A 90° dual-head SPECT system with two scanning point sources

Martín et al. [34] used a newer transmission imaging device (Beacon^{TM}) [35] that consisted of two moving ^{133}Ba sources that were contained in an assembly fixed to the detector heads (see Figure 7).
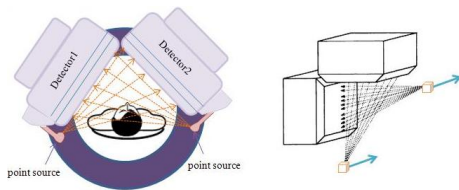

Fig 7. Illustration of dual-head Beacon transmission imaging device. This system consists of two ^{133}Ba point sources that are moving during the scan along the broader of the heads [35, 36].

The purpose of this study was to measure the additional radiation dose caused by two ^{133}Ba transmission sources. Because of the ^{133}Ba medium energy (356 keV), the emitted photons can penetrate through the septa of LEHR collimators and thereby, the transmission scans substantially have a higher resolution in compared with other transmission sources used. On the other hand, ^{133}Ba has a long-half life (10.54 years) which is useful since it avoids the replacement of the transmission source. In order to reduce the patient exposure, a thin sheet of Tantalum foil was placed over the exit slit of the source holder, which effectively filtered the low-energy photons without significantly attenuating the desired 356 keV photons.

The results of this study showed that the absorbed doses due to ^{133}Ba transmission sources used for routing attenuation correction in SPECT MPI are lower than those obtained with other transmission sources used, and also in comparison with those generated by injected radiopharmaceutical.

4.7. A triple-head SPECT system with two scanning point sources

Dondi et al. [37] performed SPECT MPI using a three-headed commercial system (IRIX, Philips Medical Systems) that had been equipped with LEHR parallel-hole collimators and two ^{133}Ba point sources (see Figure 8). Similar to the previous protocol, the two sealed sources are contained in an assembly which has been permanently fixed to the border of two of the three heads.
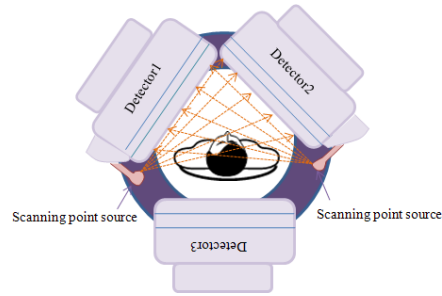

Fig 8. Illustration of triple-head Beacon transmission imaging device. The detector heads 1 and 2 are separated by an angular of 102°, while head 3 is positioned at 120° and not used for acquisition. Two ^{133}Ba point sources fixed to the borders are moving during the scan and providing transmission data required to produce attenuation map [36].

These sources can move along the border of the two detectors and produce an external transmission beam on the opposite detector. In this protocol, the acquisition was performed at three stages: (1) the Emission Stage, in which data acquisition is carried out only using heads 1 and 2, equipped with LEHR collimators, and a non-circular orbit over a total of 204°, with a step and shoots motion. Sequentially, (2) the Transmission Stage, in which data acquisition is carried out using the same way of the emission acquisition. Finally, (3) the Calibration Stage that consisted of a blank scan, required to calculate the correction factor map. This investigation demonstrated that in all of the patients under study (297 males and 203 females), the specificity and the normalcy rate increase significantly by applying of the attenuation correction. But, the sensitivity doesn't show significant change. Also, the results of this study showed that the attenuation correction increases the rate of normal reports. Of course, this increment was more striking in males than in females.

DISCUSSION

Soft-tissue attenuation is one of the potential problems in myocardial perfusion imaging which can lead to decrease capability of the diagnosis of coronary artery diseases. Several types of the camera geometries and the external source configurations have been offered by the different investigative groups for attenuation correction of SPECT MPI. In the broad class of these investigations, ^{153}Gd has been used as the external source. However, in number of the studies, ^{241}Am, ^{99m}Tc and ^{133}Ba have been used. In this paper, we reviewed different configurations used for attenuation correction of cardiac SPECT studies (see Table 3):

Table 3: Different configurations of attenuation correction with external sources for MPI.

Author	System	Transmission Source	Type of Source	Arrangement of Camera	Acquisition Mode
Ficaro	Picker	^{241}Am	a fixed line source	triple-head	simultaneous
Matsunari	Siemens	^{241}Am	a fixed line source	triple-head	simultaneous
Vidal	Picker	^{99m}Tc	a fixed line source	triple-head	simultaneous
Kluge	ADAC	^{153}Gd	two scanning line sources	dual-head	simultaneous interleaved
Gallowitsch	Elscint	^{153}Gd	two scanning line sources	dual-head	simultaneous
Almquist	ADAC	^{153}Gd	two scanning line sources	dual-head	simultaneous
Hendel	ADAC	^{153}Gd	two scanning line sources	dual-head	simultaneous
Links	SMV	^{153}Gd & ^{99m}Tc	two scanning line sources	dual-head	simultaneous and simultaneous interleaved
Harel	SMV	^{153}Gd	two scanning line sources	dual-head	simultaneous interleaved
Gibson	ADAC	^{153}Gd	two scanning line sources	dual-head	simultaneous
Velidaki	Optima NX	^{153}Gd	two scanning line sources	dual-head	simultaneous interleaved
Slart	Siemens	^{153}Gd	multiple line sources	dual-head	simultaneous interleaved
Benjamin	GE 400 AC/T	^{99m}Tc	a collimated sheet source	single-head	sequential
Kojima	GCA 7200A	^{99m}Tc	a uncollimated sheet source	dual-head	sequential
Martín	Beacon™ (Philips)	^{133}Ba	two scanning point sources	dual-head	sequential
Dondi	Beacon™ (Philips)	^{133}Ba	two scanning point sources	triplet-head	sequential

(1) A fixed line source with the fanbeam collimator on a triple-detector system,

(2) Two scanning line sources with the parallel-hole collimator on 90° dual-head systems,

(3) An array of line sources with the parallel-hole collimator on 90° dual-detector systems,

(4) A large collimated sheet-source with the parallel-hole collimator on the opposite single-detector,

(5) A small uncollimated sheet-source with an asymmetric fan-beam (AsF) collimator on the opposite head of 180° dual-detector system and a parallel-hole collimator on the other head.

(6) Two scanning point sources with the parallel-hole on dual- and triple-detector systems (Beacon transmission system).

Each configuration has unique advantages and limitations. In the configuration 1, the use of a fixed line source combined with a fan-beam collimator results in the effective acquisition of the transmission data by using of low source activity and thereby reducing the patient exposure. Although, the present of the fan-beam collimator will be effective in rejection of the scattered photons from the external line source and thereby increasing transmission image quality but, on the other hand, the limited FOV of this collimator can cause truncation artifacts because of excluding the parts of organ being imaged and may limit the accuracy of attenuation correction map. Using highly sophisticated iterative reconstruction algorithms, this problem can be minimized. In the configuration 2, the combination of a moving line source with a parallel-hole collimator leads to cover maximum FOV and thereby minimizing the likelihood of the truncation artifacts. Also, the use of two electronic windows, which move synchronously with the line sources on the opposite detectors, provides the possibility of the maximal separation of the emission and transmission data. In addition to electronic collimation (transmission detector window), in major studies performed with this configuration, the line sources is physically collimated and opened only during acquisition so that there is only a minimal radiation exposure to the patient. In the configuration 3, the multiple-line

source array used leads to production of a high continuous photon flux incoming on the each opposite detector and cover maximum FOV without need for moving the sources. However, the continuous incidence of transmission photons results in significant contamination of the emission and transmission data that thereby making impossible the use of a simultaneous acquisition mode. Advantages and drawbacks of the configuration 4 are approximately similar to the configuration 3. The main advantage of this configuration is that the source irradiates fully on the opposite detector, and therefore requires no motion of the source other than that provided by the rotation of the camera gantry.

On the other hand, the use of collimated source provides the possibility of the production of a narrow beam transmission geometry that leads to reduce the radiation dose to the patient. But the data acquisition is performed sequentially thereby increasing the imaging time and the possibility of the patient motion. In the configuration 5, the combination of a small uncollimated sheet-source with an asymmetric fan-beam collimator results in the extension of FOV for acquisition of the transmission data in comparison with the fan-beam collimator used commonly. Also, the use of this collimator results in the significant rejection of the scattered photons from source. Limitations with this configuration are non-uniformity in the peripheral FOV that may degrade the accuracy of attenuation map and also lower sensitivity of this collimator in compared with the parallel-hole collimator. The configuration 6 is a newer approach that recently has been used in the number of the investigations performed for attenuation correction. In this configuration, the medium-energy of ^{133}Ba photons provides easy penetration of these photons in the septa of low-energy parallel-hole collimator and thereby producing an attenuation map with higher resolution. However, the moving point sources used in this approach cannot produce an incident flux as uniform as the moving line sources on the each detector.

CONCLUSION

From the number of studies reviewed in this work, and also advantages and limitations mentioned for each configuration, it seems that, configuration 2 with the scanning line source geometry on 90° dual-detector SPECT systems is most appropriate and most widely implemented configuration for clinical transmission acquisition.

In this review, we have confined our study to different configurations of the external source-based attenuation correction systems for SPECT imaging. An essential problem with these systems is the low activity of the transmission sources that leads to generate poor-quality attenuation maps. Moreover, if the photon energy of the transmission source is lower than that of the injected radionuclide, there is also the problem of inclusion of downscatter emission data in the attenuation map.

In the other hand, the attenuation maps generated by X-ray CT systems, because of higher transmission photon flux, include lower noise and higher resolution, leading to higher quality. However, in hybrid SPECT/CT systems, the alignment of SPECT/CT fusion images is important, because patient movement or mechanical misalignment of the SPECT/CT system can result in misregistration. Of course, the software tools used for reregistration of misaligned studies can help to compensate this problem.

REFERENCES

1. Zaidi H. Quantitative analysis in nuclear medicine imaging. New York: Springer Science+Business Media, Inc.; 2006.

2. Celler A, Dixon KL, Chang Z, Blinder S, Powe J, Harrop R. Problems created in attenuation-corrected SPECT images by artifacts in attenuation maps: a simulation study. J Nucl Med. 2005 Feb;46(2):335-43.

3. Bushberg JT, Seibert A, Leidholdt EM, Boone JM. The essential physics of medical imaging. 2nd ed, New York: Lippincott Williams & Wilkins; 2002.

4. Tsoulfanidis N. Measurement and detection of radiation. 2nd ed. New York; McGraw-Hill; 1983.

5. Ficaro EP, Fessler JA, Rogers WL, Schwaiger M. Comparison of americium-241 and technetium-99m as transmission sources for attenuation correction of thallium-201 SPECT imaging of the heart. J Nucl Med. 1994 Apr;35(4):652-63.

6. Smith NB, Webb A. Introduction to medical imaging: physics, engineering and clinical applications. New York: Cambridge University Press; 2010.

7. Hurton, Brian F. Correction for attenuation and scatter in SPECT. Alasbimn J. 2002;5(18): Article N° AJ18-5.

8. Groch MW, Erwin WD. SPECT in the year 2000: basic principles. J Nucl Med Technol. 2000 Dec;28(4):233-44.

9. Saha GB. Physics and radiobiology of nuclear medicine. 3rd ed. New York: Springer; 2006.

10. Chang LT. A method for attenuation correction in radionuclide computed tomography. IEEE Trans Nucl Sci. 1978;NS-25:638–643.

11. Powsner RA, Powsner ER. Essential nuclear medicine physics. 2nd ed. Massachusetts: Blackwell Publishing; 2006.

12. Attenuation correction. GE Medical Systems. http://www.gehealthcare.com/usen/fun_img/nmedicine/mpr_mps/docs/attcor.pdf

13. Hashimoto J, Kubo A, Ogawa K, Amano T, Fukuuchi Y, Motomura N, Ichihara T. Scatter and attenuation correction in technetium-99m brain SPECT. J Nucl Med. 1997 Jan;38(1):157-62.

14. Ficaro EP, Fessler JA, Ackermann RJ, Rogers WL, Corbett JR, Schwaiger M. Simultaneous transmission-

emission thallium-201 cardiac SPECT: effect of attenuation correction on myocardial tracer distribution. J Nucl Med. 1995 Jun;36(6):921-31.

15. Ficaro EP, Fessler JA, Shreve PD, Kritzman JN, Rose PA, Corbett JR. Simultaneous transmission/emission myocardial perfusion tomography. Diagnostic accuracy of attenuation-corrected 99mTc-sestamibi single-photon emission computed tomography. Circulation. 1996 Feb 1;93(3):463-73.

16. Matsunari I, Böning G, Ziegler SI, Kosa I, Nekolla SG, Ficaro EP, Schwaiger M. Attenuation-corrected rest thallium-201/stress technetium 99m sestamibi myocardial SPECT in normals. J Nucl Cardiol. 1998 Jan-Feb;5(1):48-55.

17. Matsunari I, Böning G, Ziegler SI, Nekolla SG, Stollfuss JC, Kosa I, Ficaro EP, Schwaiger M. Attenuation-corrected 99mTc-tetrofosmin single-photon emission computed tomography in the detection of viable myocardium: comparison with positron emission tomography using 18F-fluorodeoxyglucose. J Am Coll Cardiol. 1998 Oct;32(4):927-35.

18. Vidal R, Buvat I, Darcourt J, Migneco O, Desvignes P, Baudouy M, Bussière F. Impact of attenuation correction by simultaneous emission/transmission tomography on visual assessment of 201Tl myocardial perfusion images. J Nucl Med. 1999 Aug;40(8):1301-9.

19. Kluge R, Sattler B, Seese A, Knapp WH. Attenuation correction by simultaneous emission-transmission myocardial single-photon emission tomography using a technetium-99m-labelled radiotracer: impact on diagnostic accuracy. Eur J Nucl Med. 1997 Sep;24(9):1107-14.

20. Gallowitsch HJ, Sykora J, Mikosch P, Kresnik E, Unterweger O, Molnar M, Grimm G, Lind P. Attenuation-corrected thallium-201 single-photon emission tomography using a gadolinium-153 moving line source: clinical value and the impact of attenuation correction on the extent and severity of perfusion abnormalities. Eur J Nucl Med. 1998 Mar;25(3):220-8.

21. Gallowitsch HJ, Unterweger O, Mikosch P, Kresnik E, Sykora J, Grimm G, Lind P. Attenuation correction improves the detection of viable myocardium by thallium-201 cardiac tomography in patients with previous myocardial infarction and left ventricular dysfunction. Eur J Nucl Med. 1999 May;26(5):459-66.

22. Almquist H, Arheden H, Arvidsson AH, Pahlm O, Palmer J. Clinical implication of down-scatter in attenuation-corrected myocardial SPECT. J Nucl Cardiol. 1999 Jul-Aug;6(4):406-11.

23. Hendel RC, Berman DS, Cullom SJ, Follansbee W, Heller GV, Kiat H, Groch MW, Mahmarian JJ. Multicenter clinical trial to evaluate the efficacy of correction for photon attenuation and scatter in SPECT myocardial perfusion imaging. Circulation. 1999 Jun 1;99(21):2742-9.

24. Hendel RC, Selker HR, Heller GV. The impact of attenuation correction and gating on SPECT perfusion imaging in patients presenting to the emergency department with chest pain [abstract]. Circulation. 2000;102:II–543.

25. Links JM, Becker LC, Rigo P, Taillefer R, Hanelin L, Anstett F, Burckhardt D, Mixon L. Combined corrections for attenuation, depth-dependent blur, and motion in cardiac SPECT: a multicenter trial. J Nucl Cardiol. 2000 Sep-Oct;7(5):414-25.

26. Harel F, Génin R, Daou D, Lebtahi R, Delahaye N, Helal BO, Le Guludec D, Faraggi M. Clinical impact of combination of scatter, attenuation correction, and depth-dependent resolution recovery for (201)Tl studies. J Nucl Med. 2001 Oct;42(10):1451-6.

27. Gibson PB, Demus D, Noto R, Hudson W, Johnson LL. Low event rate for stress-only perfusion imaging in patients evaluated for chest pain. J Am Coll Cardiol. 2002 Mar 20;39(6):999-1004.

28. Velidaki A, Perisinakis K, Koukouraki S, Koutsikos J, Vardas P, Karkavitsas N. Clinical usefulness of attenuation and scatter correction in Tl-201 SPECT studies using coronary angiography as a reference. Hellenic J Cardiol. 2007 Jul-Aug;48(4):211-7.

29. Slart RH, Que TH, van Veldhuisen DJ, Poot L, Blanksma PK, Piers DA, Jager PL. Effect of attenuation correction on the interpretation of 99mTc-sestamibi myocardial perfusion scintigraphy: the impact of 1 year's experience. Eur J Nucl Med Mol Imaging. 2003 Nov;30(11):1505-9.

30. E.COM Profile Attenuation Correction - Siemens Medical Solutions. www.medical.siemens.com/siemens/en_GB/gg_nm/Qun atitative5.pdf

31. Tsui BM1, Gullberg GT, Edgerton ER, Ballard JG, Perry JR, McCartney WH, Berg J. Correction of nonuniform attenuation in cardiac SPECT imaging. J Nucl Med. 1989 Apr;30(4):497-507.

32. Tan P, Bailey DL, Meikle SR, Eberl S, Fulton RR, Hutton BF. A scanning line source for simultaneous emission and transmission measurements in SPECT. J Nucl Med. 1993 Oct;34(10):1752-60.

33. Kojima A, Tomiguchi S, Kawanaka K, Utsunomiya D, Shiraishi S, Nakaura T, Katsuda N, Matsumoto M, Yamashita Y, Motomura N, Ichihara T. Attenuation correction using asymmetric fanbeam transmission CT on two-head SPECT system. Ann Nucl Med. 2004 Jun;18(4):315-22.

34. Martin G, Marin MD, Corredoira E, Plaza R, Navarro T, Tellez de Cepeda M, Martín Curto LM. Contribution in patient dosimetry of Ba-133 external sources in myocardial perfusion SPECT with attenuation correction. http://irpa11.irpa.net/pdfs/4d11.pdf

35. Staelens S: Monte Carlo simulations for system modeling in emission tomography. PhD thesis. Gent University; 2005. http://hdl.handle.net/1854/LU-470785

36. Beekman FJ, Kamphuis C, Hutton BF, van Rijk PP. Half-fanbeam collimators combined with scanning point sources for simultaneous emission-transmission imaging. J Nucl Med. 1998 Nov;39(11):1996-2003.

37. Dondi M, Fagioli G, Salgarello M, Zoboli S, Nanni C, Cidda C. Myocardial SPECT: what do we gain from attenuation correction (and when)? Q J Nucl Med Mol Imaging. 2004 Sep;48(3):181-7.